Explosion behavior of methane - dimethyl ether /air mixtures

Bo Zhang[1,2†], Hoi Dick Ng[3]

[1] East China University of Science and Technology
State Environmental Protection Key Laboratory of Risk Assessment and Control on Chemical Process, Shanghai, 200237, China

[2]Beijing Institute of Technology
State Key Laboratory of Explosion Science and Technology, Beijing, 100081, China

[3] Concordia University
Department of Mechanical and Industrial Engineering
Montréal, H3G 1M8, Canada

[†]Corresponding Author

E-mail: bzhang@ecust.edu.cn

Tel.: (86) 21-64253132
Fax: (86) 21-64253404

Explosion behavior of methane - dimethyl ether /air mixtures

Bo Zhang , Hoi Dick Ng

Abstract

In this study, the effect of dimethyl ether (DME) addition on the explosion of methane/air mixture is investigated. In particular, the explosion and deflagration parameters of various CH_4-DME/air mixtures are systematically studied. Those parameters include flammability limits, maximum explosion pressure, p_{max}, maximum rate of pressure rise $(dp/dt)_{max}$, and laminar burning velocity S_L. In general, the experimental results indicate that both p_{max} and $(dp/dt)_{max}$ increase with increasing DME content in the total fuel. Simple correlations to evaluate the dimensionless pressure ($\overline{p}$) of CH_4-air and DME-air mixtures with an initial pressure of 100 kPa are developed and given respectively by $\overline{p}$ =1/[2.81839+0.22424χ_{CH4}-2.14347$ln(\chi_{CH4})$] and $\overline{p}$ = 1/[1.04153+0.12637χ_{DME} -0.94532$ln(\chi_{DME})$] where χ is the volume fraction of the fuel. The experimental results also indicate that for lean CH_4 mixtures, the relationship between p_{max} and DME concentration exhibits an inversely "*U*-shaped" curve. In contrast, an exponential decay of p_{max} with increasing DME concentration is observed for rich CH_4 mixtures. By adding DME into the CH_4-air mixture, both the lower and upper flammability limits go down. The maximum amount of the total fuel for the binary blend (CH_4 plus DME) below which the mixture can be initiated is approximately 15~16%. Lastly, a good agreement is found in the determination of the laminar burning velocity S_L using both a theoretical model and the CHEMKIN-PREMIX simulation. For CH_4-DME/air mixtures, the S_L near the stoichiometric equivalence ratio φ_{total} = 1 is larger than the fuel lean or rich side. It is found that with a slight amount of DME adding into the lean CH_4 mixture, making φ_{total} closer to stoichiometry, the value of S_L increases. However, with further addition of DME into lean CH_4 mixture, or DME adding into rich CH_4 mixture, only a decreasing behavior of S_L is observed.

Keywords: Dimethyl ether addition; Maximum explosion pressure; Maximum rate of pressure rise; Flammability limits; Laminar burning velocity

1 Introduction

Alternative fuels with the properties of high-efficiency and low-emission combustion, have received particular interests because of the rapid increase in energy consumption and increasingly stringent emission regulations. Among them, natural gas (NG) is one of the most widely used alternative fuels for automobiles and has long been considered as a promising alternative fuel due to its favorable chemical characteristics, such as: high H/C ratio, large octane number, and especially its low emissions [1-3]. Methane CH_4 as an environmental-friendly fuel and the main component of NG produces less carbon dioxide for each unit of heat released, but more heat per mass unit than other complex hydrocarbons. Nonetheless, methane has some drawbacks regarding its combustion properties, e.g., long ignition delay time, low flame speed, low ignitability and narrow flammability limit range. All of these pose great challenges for its wide utilization in combustion engines [4]. However, using more reactive fuel additives, the ignition and combustion performance of methane could be greatly enhanced. From studies conducted by Dagaut [5, 6] and Yao et al. [7, 8] on the detailed chemical mechanism for low and high temperature DME oxidation and the effect of DME addition to methane for homogeneous charge compression ignition (HCCI) engines, respectively, DME has shown promise as an effective promoter of high temperature methane ignition. Due to an increasing interest in using NG in the automotive industry, a thorough understanding of the fundamental explosion and combustion characteristics of DME-added mixtures is therefore important for developing advanced, NG-based, combustion engines and corresponding operating strategies [4].

Fundamental combustion properties, such as laminar flame speed and Markstein length, have been extensively studied in the past for methane- [9-11] and DME-air mixtures [12-18]. Many studies have been performed on CH_4/H_2 or CH_4/DME binary fuel blends regarding the ignition delay time [4, 19-22], internal combustion engine ICE performance [23-25], and laminar flame speed [26-28]. The effects of DME addition on the high temperature ignition and burning properties of methane-air mixtures were also studied experimentally and numerically [19]. Premixed and

non-premixed ignition of methane/DME binary fuel blends with hot air has been studied through numerical simulation with detailed chemistry and various thermodynamic as well as transport properties [4].

While the combustion characteristics of methane mixtures with DME addition have been studied extensively, comparatively little explosion safety data, e.g., maximum explosion pressure, p_{max}, maximum rate of pressure rise $(dp/dt)_{max}$, flammability limits, and laminar burning velocity S_L, are currently available. In fact, the explosion hazard of CH_4-DME mixtures, within storage infrastructures, is high due to the large destructive energy release associated with the combustion phenomenon. Therefore, in this study, experiments are performed systematically to address the explosion safety problems of CH_4-DME/air mixtures by recording overpressure histories at different composition of CH_4 and DME in a standard 20-L spherical vessel and analyzing various derived explosion parameters. The data obtained in this study can contribute to a better understanding of the explosion behavior of CH_4-DME/air mixtures.

2 Experimental details

Measurement of the explosion parameters in CH_4-DME/air mixtures were carried out in a standard 20-L explosion spherical vessel according to the international standard ISO6184-1. A schematic of the apparatus is shown in Fig. 1. This facility was used previously for the same type of measurement for other gaseous fuels (e.g., natural gas) and detailed information of the experimental details can be found in [29] . In brief, the 20-L explosion spherical vessel consists of an explosion chamber, an electric ignition system, a control unit, a data acquisition system, a release valve, a vacuum pump and an air pump. A high-voltage electric spark was used to supply the ignition energy as in our previous studies [30-39]. The igniter was mounted at the center of the spherical bomb and a spark energy of 10 J, estimated from 1/2 CV^2 ("C" and "V" refer the capacitance and voltage, respectively. $C = 0.1102\times10^{-3}$ F, $V = 426$ Volts), was delivered by an electric ignition system.

For the explosion experiments, gas concentrations were regulated by the method of partial

pressure. The purities of the CH_4 and DME used in this experiment were 99.9% and 99.8%, respectively. The air used in the experiment is of 21% oxygen and 79% nitrogen (by volume). The experiments were performed at initial pressure of 100 kPa and temperature of 298 K. During the experiments, the explosion pressure evolutions were measured by a PCB pressure transducer installed in the vessel wall and recorded by a data acquisition system for each shot. These data yielded raw values of the explosion pressure and rate of pressure rise. In the present study, at least three shots were repeated at the same initial condition of the experiment, and five or more shots were made for the mixtures near LFL and UFL. Thus, the LFL and UFL were determined if half shots indicated explosion occur.

3 Results and discussion

3.1 Maximum explosion pressure and maximum rate of pressure rise

Samples of pressure traces obtained from experiments are shown in Fig. 2. In Fig. 2, p_{max} occurs at the peak of the curve, however, $(dp/dt)_{max}$ represents the most steep of the curve, the maximum of those parameters do not occur at the same place. To characterize the mixtures, λ is defined as the ratio of DME over the total fuel (i.e., CH_4 plus DME) as follows:

$$\lambda = \frac{C_{DME}}{C_{DME} + C_{CH4}} \quad (1)$$

in which C_{CH4} and C_{DME} denote the CH_4 and DME concentration, respectively. λ varies from 0 (pure CH_4) to 1 (pure DME). Unless specified, the total fuel is at the stoichiometric concentration with air. It can be seen from Fig. 2 that the maximum explosion pressure p_{max} increases with λ. It should be noted again that the φ_{total} (equivalence ratio of the overall fuels over air) is kept to 1 as λ changes. The slope of the pressure history is also observed to become more steep or in other words, the maximum rate of pressure rise $(dp/dt)_{max}$ increases as well with increasing λ. Figure 3 summarizes the p_{max} and $(dp/dt)_{max}$ versus λ at an initial pressure p_0 = 100 kPa. It shows clearly that p_{max} and $(dp/dt)_{max}$ increase with increasing DME content in the total fuel.

For pure CH_4-air and DME-air mixtures, the maximum explosion pressure at different fuel concentrations are shown in Fig. 4 and Fig. 5, respectively. The dimensionless pressure p_{max}/p_0 has a maximum value slightly above the stoichiometric concentration (C_{CH4} = 9.5% at $\varphi \sim 1.0$). The experimental data and the curve fit of the dimensionless pressure at different CH_4 concentration are shown in Fig. 4. The dimensionless pressure ($\overline{p}$) at different CH_4 volume fraction is correlated by the following equation:

$$\overline{p} = \frac{1}{2.81839 + 0.22424x_{CH4} - 2.14347ln(x_{CH4})} \quad (2)$$

where, $\overline{p} = p_{max} / p_0$, x_{CH4} is the volume fraction of CH_4 in air. The coefficient of determination R^2 equals to 0.9026. It should be noted that Eq. (2) is only valid for the initial pressure of 100 kPa and temperature of 298 K. It is noteworthy that, although both C and χ are essentially representing the volume fraction, C denotes the volume fraction of one fuel (either DME or CH_4) in binary fuel blends, whereas, χ is the fuel volume fraction for the mixture that contains only one fuel.

A similar plot of the dimensionless pressure versus DME concentration at 100 kPa and 298 K is shown in Fig. 5. The peak of p_{max} appears at the DME concentration C_{DME} of 7%, which is slightly larger than the stoichiometric concentration (C_{DME} = 6.54% at φ = 1). This behavior is similar to the CH_4-air mixture. The dimensionless pressure at different DME volume fraction is given by the following expression:

$$\overline{p} = \frac{1}{1.04153 + 0.12637x_{DME} - 0.94532ln(x_{DME})} \quad (3)$$

where, x_{DME} is the volume fraction of DME in air, the coefficient of determination R^2 equals to 0.9217.

Measurements of the maximum explosion pressure of CH_4-DME binary fuel blends with air are also performed in this study. In the experiment, the variation of the fuel composition was done by adding or reducing the composition of DME, at a constant amount of CH_4 (e.g., 0%, 2%, 4%,

etc.) for each text matrix. The measured maximum explosion pressures for CH_4-DME/air mixtures are shown in Fig. 6. Fig. 6a shows that the relation between p_{max} and DME concentration is an inversely "*U*-shaped" behavior. The peak of each curve moves to the left side as the amount of CH_4 increases from 2 % to 8 %. Numerical values of these peaks are given in Table 1 and compared with the data of pure CH_4-air and DME-air mixtures. It is found that the peak of p_{max} occurs at an equivalence ratio of the total fuel φ_{total} slightly larger than 1 (i.e., between 1.08 to 1.22). For a mixture with a larger amount of CH_4 and less DME addition, the value of p_{max} decreases.

However, as the equivalence ratio φ_{CH4} is larger than 1, the relation between p_{max} and DME concentration is completely different. An exponential decay curve is observed as shown in Fig.6b. This can be explained by the fact that adding DME makes the mixture even more fuel rich condition. For example, the values of φ_{total} are 1.77 and 1.66 for C_{CH4} = 10% with C_{DME} = 4%, and C_{CH4} = 12% with C_{DME} = 2%, respectively. Consequently, the corresponding p_{max} values become relatively small, merely of 0.32 MPa and 0.30 MPa, respectively.

The chemical equilibrium values of p_{max} are obtained using the GASEQ equilibrium software [40] to compare with experimental results as shown in Figs.3-6. Large discrepancy can be seen as the condition of the LFL and UFL is approached. The theoretical maximum explosion pressure from GASEQ is based on the hypothesis of ideal adiabatic explosion without losses. As the composition approaches to fuel lean and rich sides, heat loss and also incomplete reaction can significantly affect the explosion process making the phenomenon non-ideal. It is thus expected that a large discrepancy occurs between the measured results from experiment with the calculation of ideal adiabatic explosion using chemical equilibrium [41]. For some cases, the experimental data of p_{max} are larger than that from GASEQ, e.g., near the stoichiometric condition of DME-air (see Fig.5). This may be possibly due to the error of experimental measurement and other possible transient effect. Nevertheless, these two sets of data are close if the measurement uncertainty is taken into account. In general, the GASEQ data are larger than experimental results at off-stoichiometric conditions.

196 The above analysis indicates that the behavior between p_{max} and DME concentration depends
197 on the equivalence ratio of CH_4. For $\varphi_{CH4} < 1$, the behavior exhibits an inversely "*U*-shaped" curve,
198 whereas for $\varphi_{CH4} > 1$, an exponential decay curve is found.
199
200 **3.2 Flammability limits**
201 At the ambient condition of 100 kPa and 298 K, the LFL and UFL of CH_4/air determined from this
202 study are 5% and 15%, respectively. For DME/air mixture, the LFL and UFL are 3.5% and 19%,
203 respectively. It is noteworthy that the flammability limits for the CH_4-air mixture obtained in this
204 study agree well with the result published in a previous study (4.9% and 15.9%) [42]. For the
205 DME-air mixture, Mogi et al.[43] reported that the flammability limits were 4% and 13% obtained
206 using an explosion vessel with an internal volume of 180 L. A noticeable discrepancy is thus found
207 on the rich limit, and the size of the chamber appears to be an influencing factor on the
208 flammability limits, as argued by Zhang et al.[44]. This difference may be explained by the fact that
209 in the small-scale apparatus, acoustic disturbance reflected from the chamber wall may generate
210 turbulent fluctuations facilitating the flame propagation, hence prolonging the explosion limit.
211 Other effect such as the mixture inhomogeneity and cooling effect for a higher volume in the large
212 chamber vessel may also cause the observed discrepancy. It is worth noting that another study by
213 Chen et al. [45] reported the flammability limits of 4% and 17% for DME-air mixtures using a
214 smaller chamber, which indeed approach to the findings of this study.
215 Comparatively the flammability limits of DME/air are broader than CH_4/air mixture. For
216 blended CH_4-DME/air mixtures, the results are tabulated in Table 2. It is found that the LFL and
217 UFL of one fuel decreases with increasing amount of another fuel addition, e.g., as the addition of
218 CH_4 increases to 4% in DME-air mixture, the LFL and UFL of DME decrease to 1% and 12%,
219 respectively. For DME-air mixtures, the UFL is 19%. The presence of CH_4 in a binary fuel blend
220 restricts the maximum amount of the total fuel below which the mixture can be initiated to
221 approximately 15~16%, e.g., with 4%, 6%, 8% CH_4 addition, the maximum amount of DME so the

222 mixture can be initiated is 12%, 10% and 8%, respectively. Hence, these results show that CH_4 has
223 a significant effect on the flammability of DME and controls the flammable range of the binary fuel
224 blends.

225 Again, the experimental results indicate that the flammability limits for CH_4-air mixtures at the
226 initial condition of 100 kPa and 298 K are 5% for LFL and 15% for UFL. From the present data, it
227 is interesting to note that the width of the flammable area (i.e., the difference between LFL and
228 UFL) of the binary fuel blends is predominantly controlled by that of CH_4-air. For example, only a
229 shift rather than a widening or narrowing of the flammable range occurs as a small amount of DME
230 is added into the CH_4-air mixture. Equivalently, a small addition of CH_4 has a more prominent
231 effect on the flammable range of the DME-air mixture. Without any CH_4 addition, it is already
232 noted that the flammability limits of the pure DME-air mixture are 3.5% and 19%, comparatively
233 wider than that of CH_4-air. However, with just a small addition of CH_4 into the DME-air mixture, it
234 is observed that the width of the flammable area reduces noticeably to that of CH_4 and further CH_4
235 addition results only in a displacement of the flammable range as in the case of DME addition into
236 the CH_4-air mixture.

237

238 **3.3 Laminar burning velocity**

239 The laminar burning velocity, $S_{L,}$ represents the rate at which the flame front propagates into the
240 unburned gas. It received particular attention not only because it is a basic physico-chemical
241 property (e.g., reactivity, diffusivity, and exothermicity) of the premixed combustible gases [46], its
242 accurate knowledge is also essential for engine design, modeling of turbulent combustion, and
243 validation of chemical kinetic mechanisms. In addition, the determination of laminar burning
244 velocity is very important for the analysis and calculations used in explosion protection [29].

245 Laminar burning velocity are computed using the PREMIX module of the CHEMKIN package
246 [19, 41, 47-49], and alternatively by a theoretical model developed by Dahoe et al. [50, 51]. For the
247 CHEMKIN-PREMIX simulation, the chemical kinetic mechanism involves 46 species and 263
248 reaction [52]. In the previous work by Chen et al.[19], equivalent PREMIX calculations of the

laminar burning velocity for DME/CH_4/air mixtures are performed, and results are in satisfactory agreement with experimental data. As for the theoretical model, the laminar burning velocity depends on p_{max} and dp/dt. The model was also used in our previous study of natural gas-air mixtures [29] and the mathematical expression is given by:

$$S_L = \frac{1}{(p_{max} - p_0)} \frac{1}{3} \left(\frac{4\pi}{3V}\right)^{-1/3} \left(\frac{p_0}{p}\right)^{1/\gamma} \left[1 - \left(\frac{p_0}{p}\right)^{1/\gamma} \times \left(\frac{p_{max} - p}{p_{max} - p_0}\right)\right]^{-2/3} \frac{dp}{dt} \quad (4)$$

where V is the vessel volume, p and p_0 are the actual pressure and initial pressure, and γ denotes the adiabatic coefficient of the unburned gas. Using Eq. (4) the value of the laminar burning velocity S_L is first calculated by the measured pressure time history (i.e., actual pressure p and dp/dt) [51, 53-55] . The fitting of the data then yields the S_L at the reference initial condition Po. Only the S_L data calculated at a flame radius greater than 6 mm are considered in order to avoid the distortion and effects associated with spark ignition [26], so that it can be considered as an ideal spherical flame propagating outward.

The laminar burning velocities computed by the above two methods for CH_4-air and DME-air at 100 kPa are given in Fig. 7. The computed results are also compared with other experimental measurement. The experimental results for DME-air mixtures are taken from Daly et al. [13] and Qin et al.[16]. For CH_4-air mixtures, results from Chen et al. [19] are used for the comparison. It can be seen from this plot both results agree well with each other. The values of S_L obtained from the theoretical model given by Eq. (4) do not differ significantly from those computed by the CHEMKIN-PREMIX simulation and previous experimental results.

Figure 8 shows the laminar burning velocities of CH_4-DME/air mixtures at 100 kPa. For the mixtures of $\varphi < 1$ (with fixed amount of C_{CH4}= 2%, 4%, 6%, 8% for each data set), the laminar burning velocity increases to a peak and subsequently decreases as the DME concentration continues to increase. For the mixtures of $\varphi > 1$ (i.e., C_{CH4} = 10% and 12%), the laminar burning velocity decreases rapidly as more DME is added. This is because for both CH_4-air and DME-air,

the values of S_L are usually highest near stoichiometric conditions. Equivalently for CH_4-DME/air mixtures, the value of S_L near $\varphi_{total} = 1$ is generally larger than on the fuel lean or rich side as well. As a small amount of DME is initially added into the CH_4 lean mixture, the equivalence ratio of the total fuel-air mixture tends toward stoichiometry, which makes S_L increase. However, if more DME is added into the lean CH_4 mixture (or DME added into the rich CH_4 mixture), S_L decreases.

4 Concluding remarks

A detailed investigation on the explosion behavior of methane - dimethyl ether /air mixture is performed in this study. The explosion and deflagration parameters including the maximum explosion pressure, maximum rate of pressure rise, flammability limits, and laminar burning velocity of the mixture are systematically measured and analyzed. Some conclusions are made as follows:

1. p_{max} and $(dp/dt)_{max}$ increase with increasing DME content λ in the total fuel. For both CH_4-air and DME-air mixtures, the dimensionless pressure at the equilibrium state has a maximum value at slightly above the stoichiometric concentration, and dimensionless pressure $\overline{p}$ can be approximated by the correlations: $\overline{p} = 1/[2.81839+0.22424\chi_{CH4}-2.14347ln(\chi_{CH4})]$ and $\overline{p} = 1/[1.04153+0.12637\chi_{DME}-0.94532ln(\chi_{DME})]$ at 100kPa, respectively.

2. The relation between p_{max} and DME concentration exhibits an inversely "*U*-shaped" curve for CH_4 lean mixture, and an exponential decay curve for CH_4 rich mixture. By adding the content of DME into CH_4-air mixture, the flammability limits are slightly extended. The maximum amount of the total fuel (CH_4 plus DME) below which the mixture can be initiated is approximately 15~16%.

3. The comparison of laminar burning velocity results between the CHEMKIN-PREMIX simulations and a theoretical model shows a satisfactory agreement for both CH_4-air and DME-air mixtures at 100 kPa. For CH_4-DME/air mixtures, S_L near $\varphi_{total} = 1$ is larger than fuel lean or rich mixtures. As initially a small amount of DME is added into the lean CH_4 mixture, the mixture φ_{total}

moves closer to 1 causing S_L to increase. Further additions of DME into the lean CH_4 mixture, or any DME added into the rich CH_4 mixture, only result in a decrease of S_L.

Acknowledgments

This work is supported by the National Natural Science Foundation of China (Grant No.: 11402092), China Postdoctoral Science Foundation (Grant No.: 2014T70403), Fundamental Research Funds for the Central Universities (Grant No.: 222201314030), and the opening project of State Key Laboratory of Explosion Science and Technology, Beijing Institute of Technology (Grant No.:KFJJ15-03M).

References

[1] Kubesh J, King SR, Liss WE. Effect of gas composition on octane number of natural gas fuels. SAE-922359, 1992.

[2] Liao SY, Jiang DM, Huang ZH, Cheng Q, Gao J, Hu Y. Approximation of flammability region for natural gas−air−diluent mixture. J Hazard Mater. 2005; 125:23-8.

[3] Tang C, Zhang S, Si Z, Huang Z, Zhang K, Jin Z. High methane natural gas/air explosion characteristics in confined vessel. J Hazard Mater. 2014; 278:520-8.

[4] Dai P, Chen Z, Chen SY. Ignition of methane with hydrogen and dimethyl ether addition. Fuel. 2014; 118:1-8.

[5] Dagaut P, Daly C, Simmie JM, Cathonnet M. The oxidation and ignition of dimethyl ether from low to high temperature (500−1600 K): Experiments and kinetic modeling. Proc. Combust. Inst. 1998; 27:361-9.

[6] Dagaut P, Boettner J, Cathonnet M. Chemical kinetic study of dimethyl ether oxidation in a jet stirred reactor from 1 to 10 atm: Experiments and kinetic modeling. Proc. Combust. Inst. 1996; 26:627-32.

[7] Yao MF, Zheng ZQ, Qin J. Experimental Study on Homogeneous Charge Compression Ignition Combustion With Fuel of Dimethyl Ether and Natural Gas. J Eng Gas Turb Powe. 2005; 128:414-20.

[8] Yao MF, Zheng ZL, Liu HF. Progress and recent trends in homogeneous charge compression ignition (HCCI)

engines. Prog Energ Combust. 2009; 35:398-437.

[9] Bosschaart KJ, de Goey LPH, Burgers JM. The laminar burning velocity of flames propagating in mixtures of hydrocarbons and air measured with the heat flux method. Combust Flame. 2004; 136:261-9.

[10] Tahtouh T, Halter F, Mounaïm-Rousselle C. Measurement of laminar burning speeds and Markstein lengths using a novel methodology. Combust Flame. 2009; 156:1735-43.

[11] Rozenchan G, Zhu DL, Law CK, Tse SD. Outward propagation, burning velocities, and chemical effects of methane flames up to 60 atm. Proc. Combust. Inst. 2002; 29:1461-70.

[12] Gabet KN, Shen H, Patton RA, Fuest F, Sutton JA. A comparison of turbulent dimethyl ether and methane non-premixed flame structure. Proc. Combust. Inst. 2013; 34:1447-54.

[13] Daly CA, Simmie JM, Würmel J, Djebaili N, Paillard C. Burning velocities of dimethyl ether and air. Combust Flame. 2001; 125:1329-40.

[14] de Vries J, Lowry WB, Serinyel Z, Curran HJ, Petersen EL. Laminar flame speed measurements of dimethyl ether in air at pressures up to 10 atm. Fuel. 2011; 90:331-8.

[15] Huang ZH, Wang Q, Yu JR, Zhang Y, Zeng K, Miao HY, Jiang DM. Measurement of laminar burning velocity of dimethyl ether-air premixed mixtures. Fuel. 2007; 86:2360-6.

[16] Qin X, Ju Y. Measurements of burning velocities of dimethyl ether and air premixed flames at elevated pressures. Proc. Combust. Inst. 2005; 30:233-40.

[17] Zhao Z, Kazakov A, Dryer FL. Measurements of dimethyl ether/air mixture burning velocities by using particle image velocimetry. Combust Flame. 2004; 139:52-60.

[18] Lu XC, Han D, Huang Z. Fuel design and management for the control of advanced compression-ignition combustion modes. Prog Energ Combust. 2011; 37:741-83.

[19] Chen Z, Qin X, Ju Y, Zhao Z, Chaos M, Dryer FL. High temperature ignition and combustion enhancement by dimethyl ether addition to methane-air mixtures. Proc. Combust. Inst. 2007; 31:1215-22.

347 [20] Gersen S, Anikin NB, Mokhov AV, Levinsky HB. Ignition properties of methane/hydrogen mixtures in a rapid
348 compression machine. Int J Hydrogen Energ. 2008; 33:1957-64.
349 [21] Tang CL, Wei LJ, Zhang JX, Man XJ, Huang ZH. Shock tube measurements and kinetic investigation on the
350 ignition delay times of methane/dimethyl ether mixtures. Energy Fuels. 2012; 26:6720-8.
351 [22] Zhang Y, Huang Z, Wei L, Zhang J, Law CK. Experimental and modeling study on ignition delays of lean
352 mixtures of methane, hydrogen, oxygen, and argon at elevated pressures. Combust Flame. 2012; 159:918-31.
353 [23] Shrestha SOB, Karim GA. Hydrogen as an additive to methane for spark ignition engine applications. Int J
354 Hydrogen Energ. 1999; 24:577-86.
355 [24] Bauer CG, Forest TW. Effect of hydrogen addition on the performance of methane-fueled vehicles. Part I: effect
356 on S.I. engine performance. Int J Hydrogen Energ. 2001; 26:55-70.
357 [25] Wang J, Chen H, Liu B, Huang Z. Study of cycle-by-cycle variations of a spark ignition engine fueled with natural
358 gas−hydrogen blends. Int J Hydrogen Energ. 2008; 33:4876-83.
359 [26] Huang ZH, Zhang Y, Zeng K, Liu B, Wang Q, Jiang DM. Measurements of laminar burning velocities for natural
360 gas−hydrogen−air mixtures. Combust Flame. 2006; 146:302-11.
361 [27] Chen Z, Dai P, Chen S. A model for the laminar flame speed of binary fuel blends and its application to
362 methane/hydrogen mixtures. Int J Hydrogen Energ. 2012; 37:10390-6.
363 [28] Chen Z. Effects of hydrogen addition on the propagation of spherical methane/air flames: A computational study.
364 Int J Hydrogen Energ. 2009; 34:6558-67.
365 [29] Zhang B, Xiu GL, Bai CH. Explosion characteristics of argon/nitrogen diluted natural gas-air mixtures. Fuel. 2014;
366 124:125-32.
367 [30] Zhang B, Ng HD, Mével R, Lee JHS. Critical energy for direct initiation of spherical detonations in $H_2/N_2O/Ar$
368 mixtures. Int J Hydrogen Energ. 2011; 36:5707-16.
369 [31] Zhang B, Ng HD, Lee JHS. The critical tube diameter and critical energy for direct initiation of detonation in

370 C_2H_2/N_2O/Ar mixtures. Combust Flame. 2012; 159:2944-53.

371 [32] Zhang B, Ng HD, Lee JHS. Measurement and scaling analysis of critical energy for direct initiation of gaseous
372 detonations. Shock Waves. 2012; 22:275-9.

373 [33] Zhang B, Ng HD, Lee JHS. Measurement and relationship between critical tube diameter and critical energy for
374 direct blast initiation of gaseous detonations. J Loss Prevent Proc. 2013; 26:1293-9.

375 [34] Zhang B, Mehrjoo N, Ng HD, Lee JHS, Bai CH. On the dynamic detonation parameters in acetylene-oxygen
376 mixtures with varying amount of argon dilution. Combust Flame. 2014; 161:1390-7.

377 [35] Zhang B, Kamenskihs V, Ng HD, Lee JHS. Direct blast initiation of spherical gaseous detonations in highly argon
378 diluted mixtures. Proc. Combust. Inst. 2011; 33:2265-71.

379 [36] Zhang B, Bai CH. Critical energy of direct detonation initiation in gaseous fuel−oxygen mixtures. Safety Sci. 2013;
380 53:153-9.

381 [37] Zhang B, Bai CH. Methods to predict the critical energy of direct detonation initiation in gaseous hydrocarbon
382 fuels -An overview. Fuel. 2014; 117:294-308.

383 [38] Mehrjoo N, Zhang B, Ng HD, Lee JHS. Response of critical tube diameter phenomenon to small perturbations for
384 gaseous detonations. Shock Waves. 2014; 24:219-29.

385 [39] Eaton R, Zhang B, Bergthorson JM, Ng HD. Measurement and chemical kinetic predictions of detonation cell size
386 in methanol-oxygen mixtures. Shock Waves. 2012; 22:173-8.

387 [40] GASEQ. 2012. A Chemical equilibrium program for windows. Available from: <www.c.morley.dsl.pipex.com/>

388 [41] Di Benedetto A, Di Sarli V, Salzano E, Cammarota F, Russo G. Explosion behavior of $CH_4/O_2/N_2/CO_2$ and
389 $H_2/O_2/N_2/CO_2$ mixtures. Int J Hydrogen Energ. 2009; 34:6970-8.

390 [42] Cashdollar KL, A Zlochower I, Green GM, Thomas RA, Hertzberg M. Flammability of methane, propane, and
391 hydrogen gases. J Loss Prevent Proc. 2000; 13:327-40.

392 [43] Mogi T, Horiguchi S. Explosion and detonation characteristics of dimethyl ether. J Hazard Mater. 2009;

164:114-9.

[44] Zhang B, Bai CH, Xiu GL, Liu QM, Gong GD. Explosion and flame characteristics of methane/air mixtures in a large-scale vessel. Process Saf Prog. 2014; 33:362-8.

[45] Chen X, Bi SS, Wu JT. The explosion limit of dimethyl ether, methane and their mixture. Journal of Engineering Thermophysics. 2009; 30:1267-70.

[46] Law CK. Combustion Physics. New York: Cambridge University Press, 2006.

[47] Kuznetsov M, Redlinger R, Breitung W, Grune J, Friedrich A, Ichikawa N. Laminar burning velocities of hydrogen-oxygen-steam mixtures at elevated temperatures and pressures. Proc. Combust. Inst. 2011; 33:895-903.

[48] Paidi SK, Bhavaraju A, Akram M, Kumar S. Effect of N_2/CO_2 dilution on laminar burning velocity of H2−air mixtures at high temperatures. Int J Hydrogen Energ. 2013; 38:13812-21.

[49] Prathap C, Ray A, Ravi MR. Investigation of nitrogen dilution effects on the laminar burning velocity and flame stability of syngas fuel at atmospheric condition. Combust Flame. 2008; 155:145-60.

[50] Dahoe AE, Zevenbergen JF, Lemkowitz SM, Scarlett B. Dust explosions in spherical vessels: the role of flame thickness in the validity of the ' cube-root law '. J Loss Prevent Proc. 1996; 9:33-44.

[51] Dahoe AE. Laminar burning velocities of hydrogen-air mixtures from closed vessel gas explosions. J Loss Prevent Proc. 2005; 18:152-66.

[52] Zhao ZW, Chaos M, Kazakov A, Dryer FL. Thermal decomposition reaction and a comprehensive kinetic model of dimethyl ether. Int J Chem Kinet. 2008; 40:1-18.

[53] Salzano E, Cammarota F, Di Benedetto A, Di Sarli V. Explosion behavior of hydrogen methane/air mixtures. J Loss Prevent Proc. 2012; 25:443-7.

[54] Di Benedetto A, Di Sarli V, Salzano E, Cammarota F, Russo G. Explosion behavior of $CH_4/O_2/N_2/CO_2$ and $H_2/O_2/N_2/CO_2$ mixtures. Int J Hydrogen Energ. 2009; 34:6970-8.

[55] Takizawa K, Takahashi A, Tokuhashi K, Kondo S, Sekiya A. Burning velocity measurement of fluorinated

416 compounds by the spherical-vessel method. Combust Flame. 2005; 141:298-307.

417

418

Tables

Table 1 The compositions of CH_4 and DME and corresponding φ at the peak value of p_{max}

Table 2 Flammability limits of CH_4-DME/air mixtures

Table 1

CH_4 / % vol.	DME / % vol.	φ_{total}	p_{max} / MPa
0	7	1.08	1.08
2	6.5	1.22	0.94
4	5	1.20	0.88
6	3	1.10	0.85
8	2	1.16	0.78
10	0	1.06	0.80

Table 2

CH_4 %vol.	LFL(DME) %vol.	UFL(DME) %vol.	DME %vol.	LFL(CH_4) %vol.	UFL(CH_4) %vol.
0	3.5	19	0	5	15
2	3	14	1	4	14
4	1	12	3	2	12
6	–	10	5	0	10
8	–	8	6.5	–	8
9.5	–	6	7	–	8
10	–	6	9	–	6
12	–	3	11	–	4
14	–	1	13	–	2
15	–	–	15	–	1

435 **Figure captions**

436

437 Fig.1 The 20-L explosion spherical vessel (1 = DME, 2 = CH_4, 3 = air)

438 Fig.2 Typical pressure trajectories for different CH_4 and DME compositions

439 Fig.3 p_{max} and $(dp/dt)_{max}$ as a function of ratio λ

440 Fig.4 p_{max} as a function of CH_4 concentration at 100 kPa

441 Fig.5 p_{max} as a function of DME concentration at 100 kPa

442 Fig.6 p_{max} as a function of DME concentration with different CH_4 composition, (a) $\varphi_{CH4} < 1$, (b)

443 $\varphi_{CH4} > 1$

444 Fig.7 Comparison of the laminar burning velocity from different methods for CH_4-air and DME-air

445 mixtures

446 Fig.8 Laminar burning velocity of CH_4-DME/air mixtures

447

448

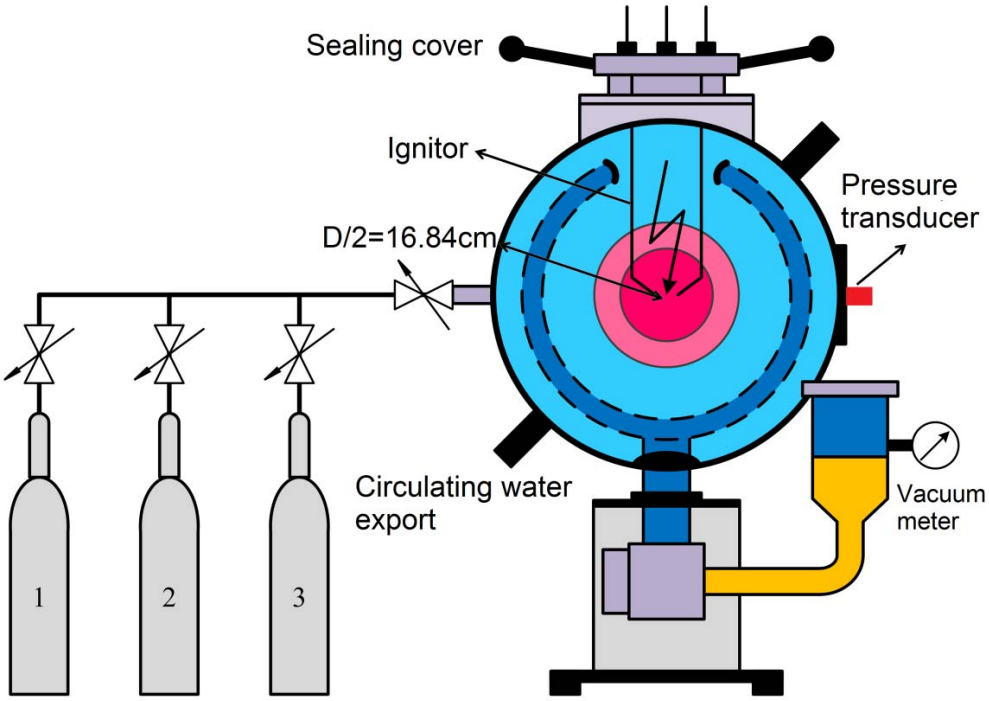
Sealing cover
Ignitor
D/2=16.84cm
Pressure transducer
Circulating water export
Vacuum meter
1
2
3

Fig.1

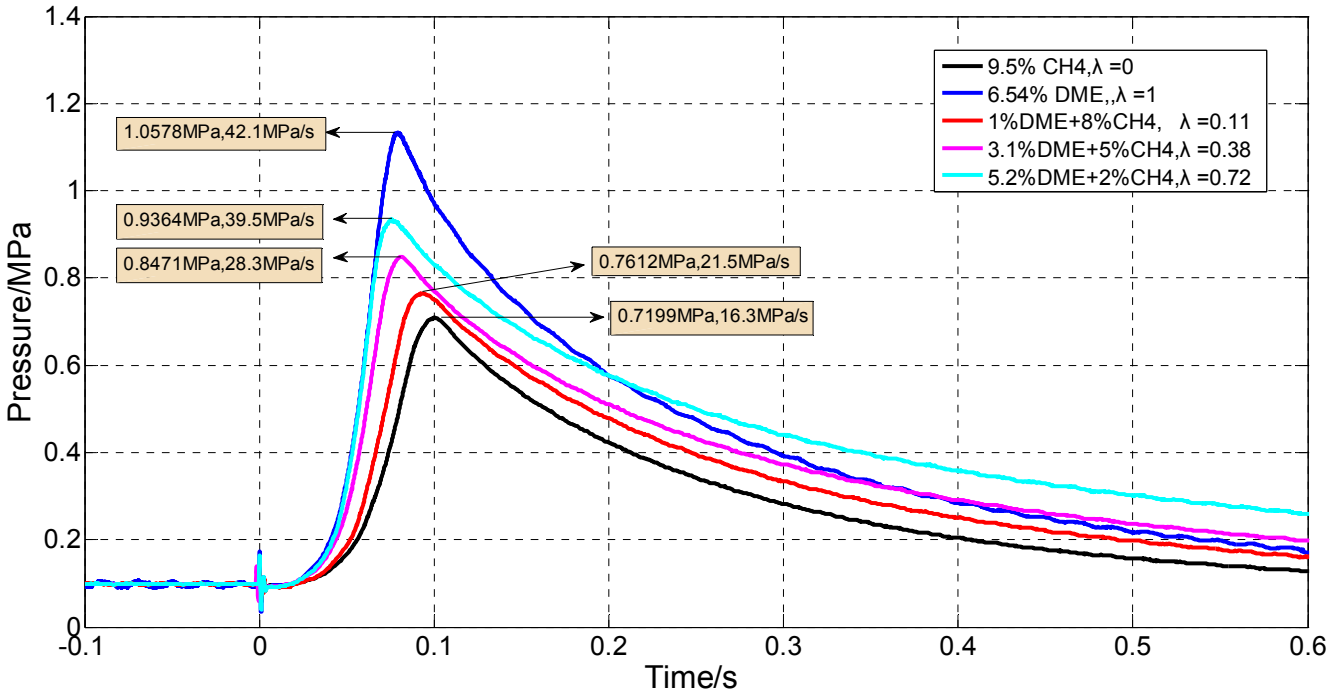
1.0578MPa,42.1MPa/s
0.9364MPa,39.5MPa/s
0.8471MPa,28.3MPa/s
0.7612MPa,21.5MPa/s
0.7199MPa,16.3MPa/s
9.5% CH4,λ =0
6.54% DME,,λ =1
1%DME+8%CH4, λ =0.11
3.1%DME+5%CH4,λ =0.38
5.2%DME+2%CH4,λ =0.72
Pressure/MPa
Time/s
1.4
1.2
1
0.8
0.6
0.4
0.2
0
-0.1
0
0.1
0.2
0.3
0.4
0.5
0.6

Fig.2

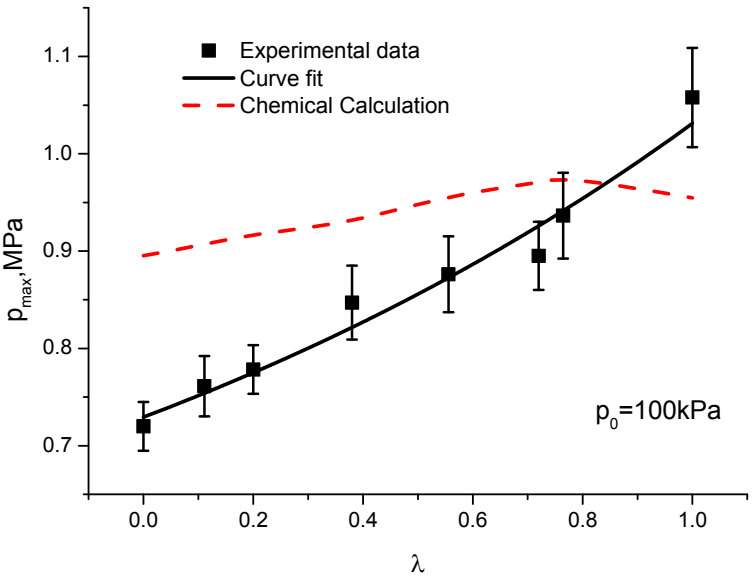
Experimental data
Curve fit
Chemical Calculation
p_{max},MPa
p_0=100kPa
λ

(a)

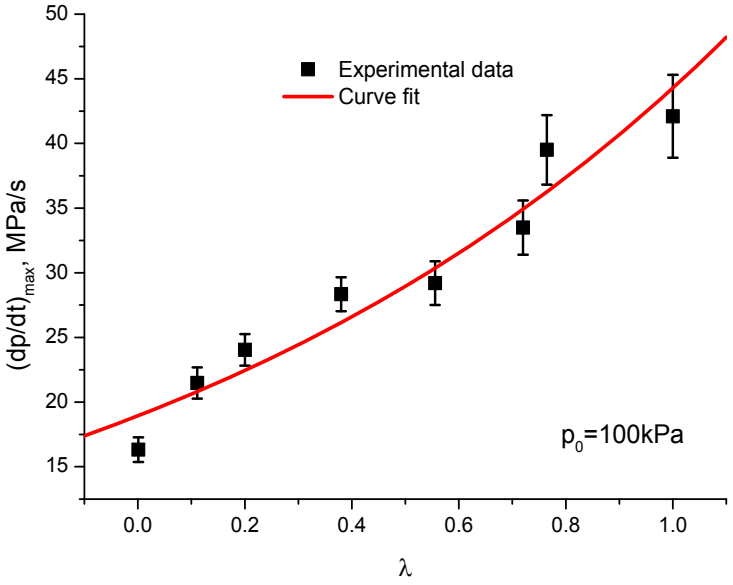
Experimental data
Curve fit
$(dp/dt)_{max}$, MPa/s
p_0=100kPa
λ

(b)

Fig.3

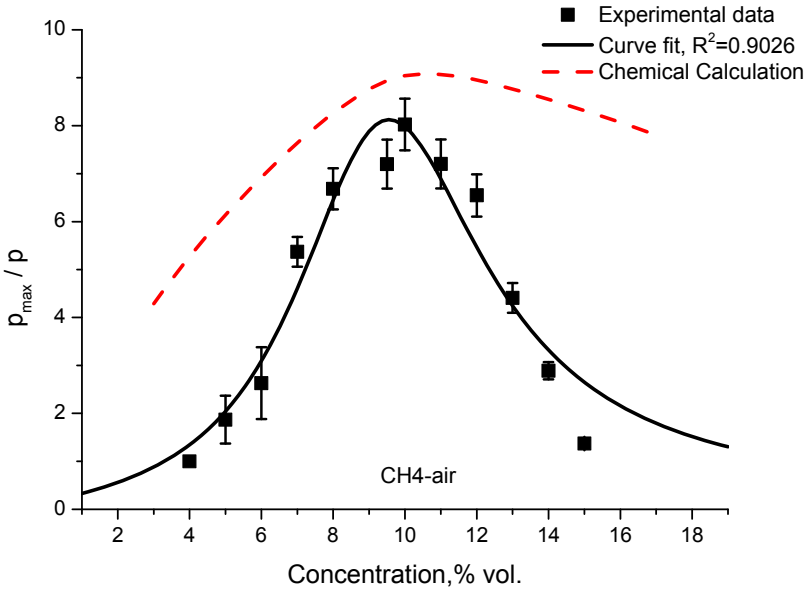
Experimental data
Curve fit, R2=0.9026
Chemical Calculation
pmax / p
CH4-air
Concentration,% vol.

Fig.4

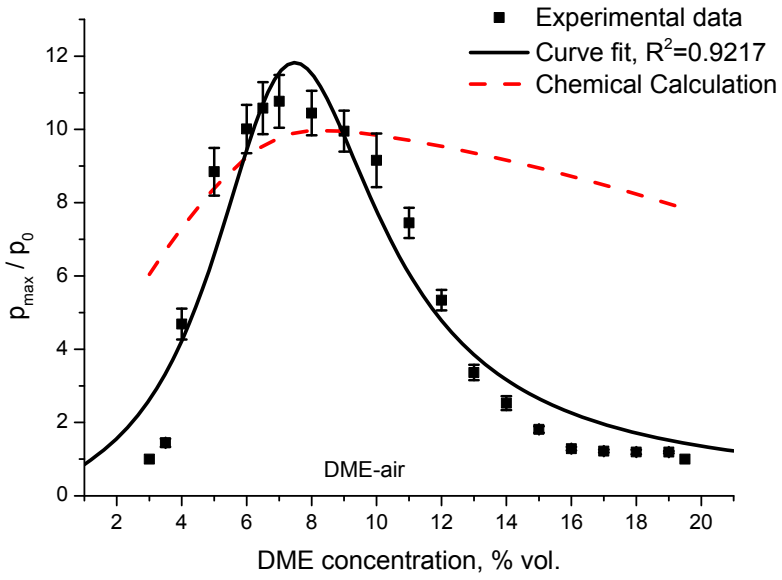
Experimental data
Curve fit, R2=0.9217
Chemical Calculation
pmax / p0
DME-air
DME concentration, % vol.

Fig.5

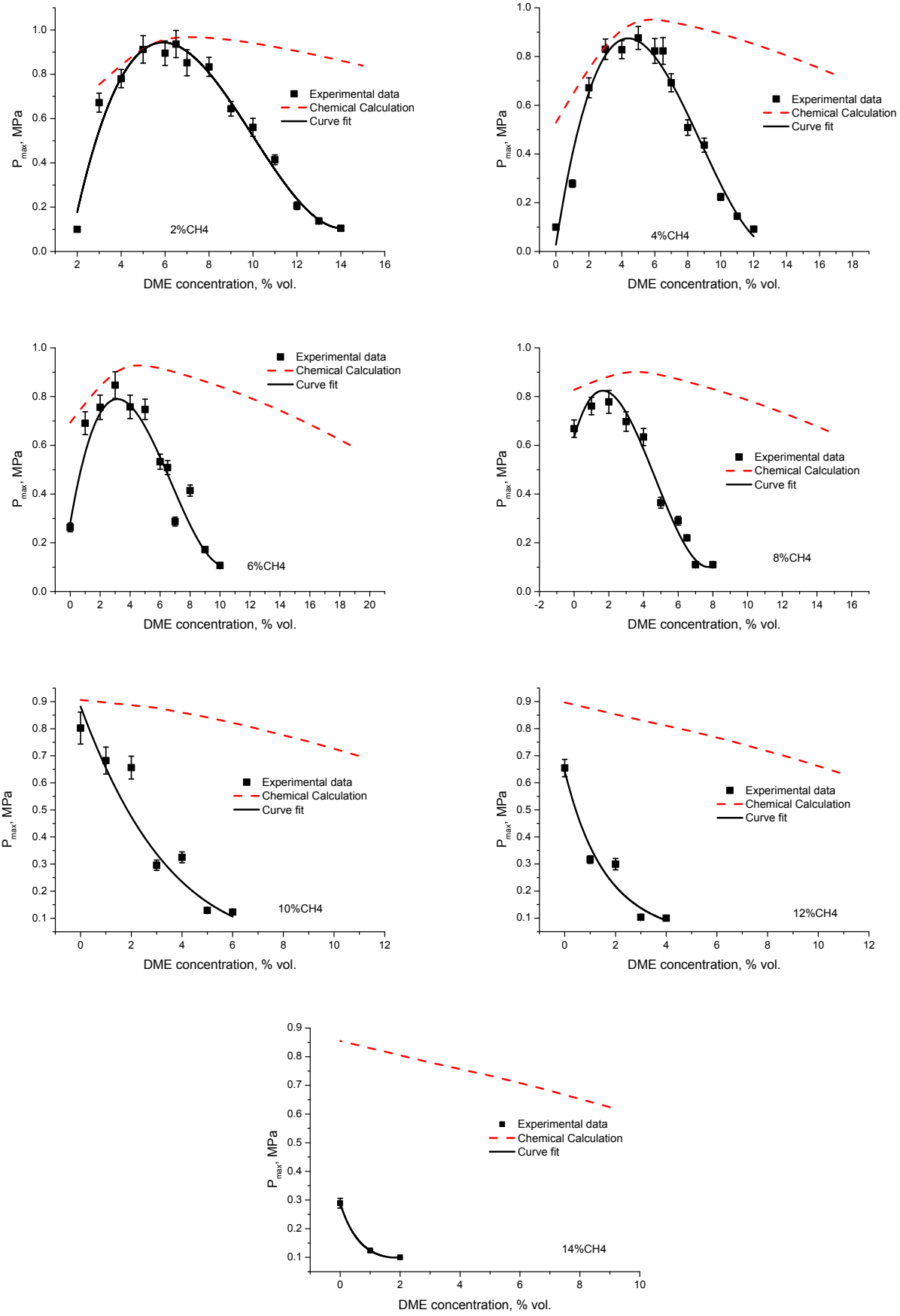
Experimental data
Chemical Calculation
Curve fit
2%CH4
4%CH4
6%CH4
8%CH4
10%CH4
12%CH4
14%CH4
P_{max}, MPa
DME concentration, % vol.

Fig.6

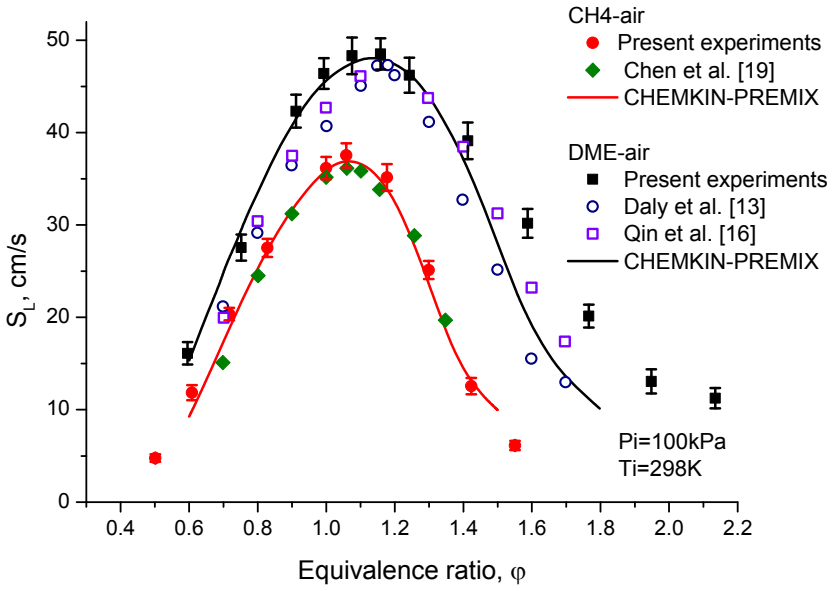
CH4-air
Present experiments
Chen et al. [19]
CHEMKIN-PREMIX
DME-air
Present experiments
Daly et al. [13]
Qin et al. [16]
CHEMKIN-PREMIX
Pi=100kPa
Ti=298K
S_L, cm/s
Equivalence ratio, φ
0
10
20
30
40
50
0.4
0.6
0.8
1.0
1.2
1.4
1.6
1.8
2.0
2.2

Fig.7

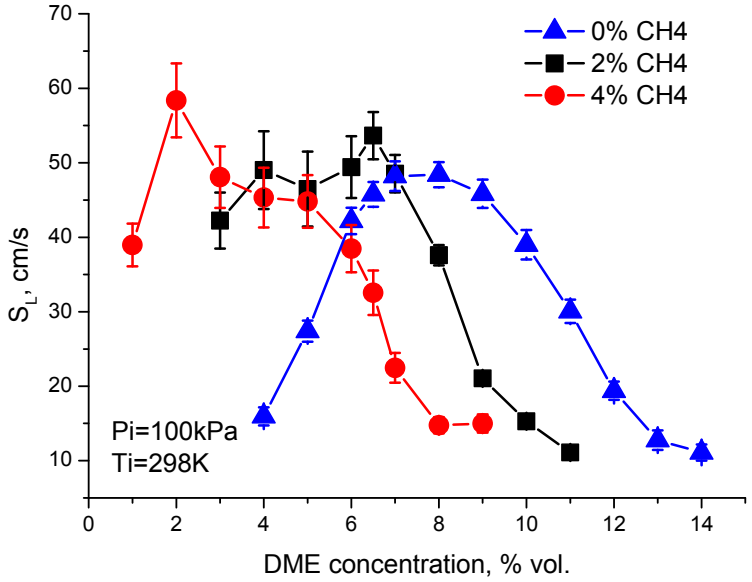
0% CH4
2% CH4
4% CH4
Pi=100kPa
Ti=298K
S_L, cm/s
DME concentration, % vol.

(a)

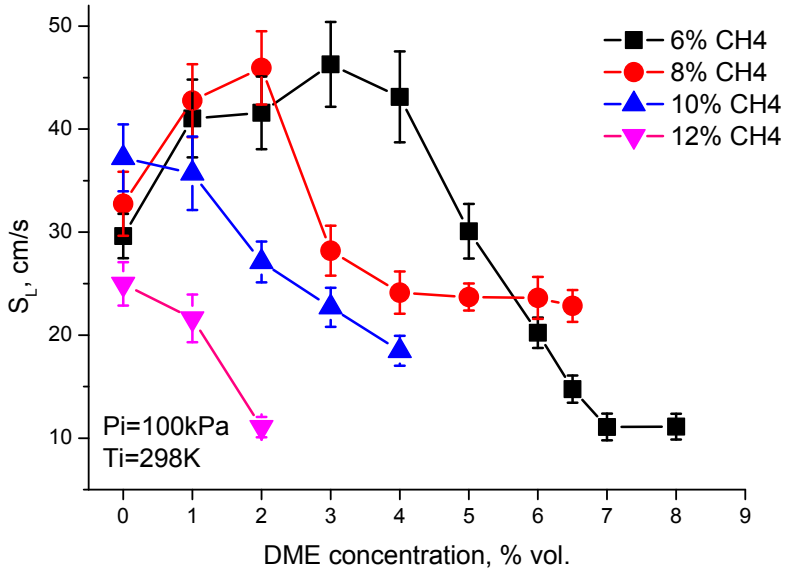
6% CH4
8% CH4
10% CH4
12% CH4
Pi=100kPa
Ti=298K
S_L, cm/s
DME concentration, % vol.

(b)

Fig.8